FPGA Based Ultrasound Backend System with Image Enhancement Technique

Vivek Akkala, P. Rajalakshmi, Punit Kumar, Uday B. Desai
Department of Electrical Engineering
IIT Hyderabad - Andhra Pradesh - 502205
Email: ee12m1041, raji, punit, ubdesai@iith.ac.in

***Abstract*—Ultrasound imaging uses high-frequency sound waves in medical imaging like obstetric diagnosis, stones in kidney etc. As ultrasound images are captured in real-time, they can show movement of the body's internal organs as well as blood flowing through blood vessels. In this paper medical B-mode architecture of the backend system is implemented in Kintex-7 FPGA platform. The backend processing consists of envelope detection which uses fixed filter coefficients for Hilbert transformation, log compression technique to achieve the desired dynamic range for display and image enhancement technique to increase the contrast. In-phase and quadrature phase components are computed using envelope detection block, whose absolute value is compressed to fit the dynamic range of display and interpolated to avoid artifacts while displaying. Further full scale contrast stretch enhancement technique is used to improve the image clarity. The implementation of the backend algorithms along with image enhancement technique on FPGA, show that the resolution of display is improved and also the hardware resource utilization is minimized leading to compact design for portable ultrasound systems.**

Keywords: Field programmable gate arrays, Programmable logic arrays, ultrasonic transducers, image quality, image enhancement.

I. Introduction

Ultrasound-based diagnostic imaging technique used for visualizing body structures, is called ultrasonography. It uses ultrasound spectrum from 1MHz to 50MHz for good resolution and good penetrating ability [1]. They are generated by converting a Radio Frequency (RF) electrical signal into mechanical vibration via a piezoelectric transducer sensor [2]. Ultrasonography interprets the echoes of high frequency sound waves sent into the biological tissue from the surface and forms the image.

The developing trend in the digital electronics lead to the development in the ultrasound systems particularly in improving the image quality and decreasing the price for implementation. Traditional ultrasound machines are not very flexible in implementing new features as they were built using multiple fixed-function circuit boards to meet high data rate requirements [3]. Design of ultrasound machines in the recent years could provide some flexibility in core ultrasound processing by using digital signal processing (DSPs). Digital processing techniques on Field Programmable Gate Array (FPGA) based ultrasound system, gives better flexibility over traditional microprocessors and DSPs in terms of implementation because of their re-configurable characteristics. The use of modern components and the flexible modular architecture has prepared the platform for adaptation to new signal-processing technologies. The FPGA configuration is generally specified using a hardware description language (HDL). FPGAs contain programmable logic components called logic blocks that can be configured to perform complex computational functions, or merely simple logic gates like AND and XOR [4].

Implementation on FPGA can miniaturize the traditional ultrasound machines. It provides high performance platform for realization of application specific ultrasound instruments and many image processing capabilities at low cost, thereby decreasing the cost of patient diagnosis. The compact design with high image quality is a very good solution to improve the health care level specifically in rural areas.

In this paper, we are focusing on FPGA implementation of the backend processing for ultrasound system. Backend processing consists of Hilbert transform, log compression to extract image information from the echoes and reduce the dynamic range, later scan conversion is applied to display the B-mode image of the tissue structure by converting the pulse echo from polar form (r,θ) to Cartesian form. Finally full scale contrast stretch image enhancement technique is implemented to improve the image contrast.

The organization of paper is as follows: in Section II, functioning of ultrasound system and image processing techniques are described. In Section III, system architecture for backend processing is discussed. Section IV reports the FPGA implementation with results and Section V concludes the paper.

II. B-Mode system

A. Acquisition System

All ultrasound systems typically consists of four main components as shown in Fig.1. The first being the transducer to transmit and receive ultrasound pulses, the second is the beam forming to condition the signal being transmitted and received. The third part consists of signal processing

techniques to process the received data with high dynamic range and finally displaying the ultrasound image.

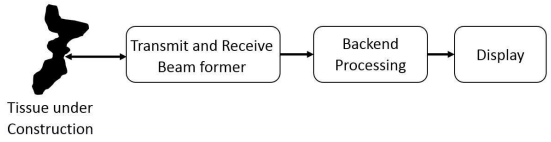

Fig. 1. Block diagram of ultrasound image acquisition system

B. B-Mode Image Processing

The RF scan-line data received are successively placed side by side resulting in the final B-Mode image. In simpler terms, it is a signal that contains the variation in the amplitude of the RF data. The RF data has its amplitude and phase similar to that of a sinusoidal. The received RF echo data by themselves carry little information about the structure of tissue being imaged. The amplitude of the sinusoidal gives the information of the reflection and back scattering at a particular depth in the tissue. Therefore the amplitude demodulation is carried out to remove the alternations, by quadrature demodulation and decimation using in-phase (I) and quadrature (Q) samples as shown in Fig. 2. The envelope of the demodulated signal having high dynamic range is detected from the RF data and should be compressed to match the dynamic range of human eye.

Fig. 2. Basic Backend processing

After log compression, scan conversion is done, which include coordinate transformation from polar to Cartesian for curvilinear and phased array probe to reduce the artifacts while displaying and also provide user interface to zoom, rotate, etc. Scan conversion includes linear interpolation and address transformation between neighbouring pixel values to smoothen the effects of co-ordinate re-sampling as discussed in [6], [7], thus avoiding unnecessary artifacts and providing better interface to user.

III. Ultrasound Backend System Architecture

After receiving the processed data from beamformer which includes delay and summation of echo signals, we started our processing with envelope detection where information of the tissue is deduced by taking the absolute value of real and quadrature components [8].

1) Envelope Detection: Traditional approach to generate I/Q data include analog/digital base band demodulation which requires significant extra circuitry on each channel. Hence Hilbert Transform is used to reduce the amount of hardware required and get accurate values of the quadrature components as it provides 90-degree phase shift at all frequencies [9]. The Hilbert transform shifts the phase of a signal by 90 degrees i.e. positive frequency components are shifted by +90 degrees, and negative frequency components are shifted by - 90 degrees. Digital FIR filter approximations are used to implement the Hilbert transformation. FIR filter for Linear Time Invariant (LTI) systems described as follows [8]

$$\begin{aligned} y[n] &= b_0x[n] + b_1x[n-1] + ... + b_Mx[n-M] \\ &= \textstyle\sum_{i=0}^{M} b_i x[n-i] \end{aligned}$$

where x is the input signal, y is the output signal and the constants b_i, $i = 0, 1, 2, ..., M$, are the coefficients. The Hilbert transformed data of the received echo signal can be generated by the above designed FIR Hilbert filter. The impulse response of the Hilbert filter with length N is defined as [10]:

$$h[n] = \begin{cases} \frac{2}{\pi}\frac{sin^2(\pi(n-\alpha)/2)}{n-\alpha} & n \neq \alpha \\ 0 & n = \alpha \end{cases}$$

$\alpha = (N-1)/2$. Filter order for FIR Hilbert filter is selected based on normalized root mean square error (RMSE) between ideal Hilbert filter and designed n-tap FIR Hilbert filter. Table 1 gives the comparison between various FIR Hilbert filters [11].

TABLE I
Normalized RMSE for FIR Hilbert filters

FIR Hilbert filter order	Normalized RMSE value
16	0.0109
20	0.0096
24	0.0092
28	0.0091
32	0.0090

2) Dynamic Range Compression: The actual dynamic range of the received signal is around 80dB or higher depending on the ADC bits of amplifier. Amplifiers are used in the front end of ultrasound systems to transform received echo signals to digital values that are used for further processing. As the maximum dynamic range of the human eye is in the order of 30 dB [12], log transformation is used to compress the pixel values having dynamic range of 80dB to desired range [13]. Hence the signal is log compressed to 8 bits to fit the dynamic range for display.

3) Reconstruction and Image Enhancement: The data obtained after dynamic range compression is in Cartesian coordinates since it is assumed that linear probes are used.

Thus, the received echoes are directly interpolated based on their neighbouring pixel values, generally 4 nearest neighbours. Superior image quality can be obtained by using linear interpolation with the original data that are sampled to match inter pixel spacing [14]. Point operations are applied on the image formed after interpolation to enhance the image clarity, where a function f operates on single pixel in image I to obtain a full scale contrast stretch image J . It is given by

$$J(i,j) = f[I(i,j)]; 0 \leq i \leq N-1, 0 \leq j \leq M-1$$

where M, N are the dimensions of the image I. Point operations provide a flat histogram as it makes rich use of available gray scale and give lots of texture over many gray levels.

IV. FPGA based Backend System Implementation and Results

Hardware software co-simulation was done to study the performance of the proposed ultrasound backend system. Computationally intensive modules such as envelope detection, log compression and scan conversion are specifically implemented on Kintex 7 FPGA platform (Fig. 3) [15] as shown in to assure that the desired output is produced.

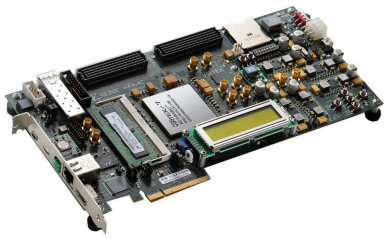

Fig. 3. Kintex 7 FPGA

The system is implemented in the hardware description language (VHDL) and synthesized with Kintex-7 FPGA, using Xilinx system generator (Xilinx, Inc.) and MATLAB Simulink (Mathworks, Inc.). RF data for backend system analysis were obtained from [16]. Following describes RF data: Ramp and hold stress stimulus were used to initiate a creep-recovery method for imaging breast lesions. Linear transducer array from Antares System is manually pressed into the skin surface in anterior-posterior direction for a time period of 12 sec. Compressive force is applied for the first second and later released for remaining time. Benign patient data downloaded is biopsy-verified and is presented with non-palpable tumours which was detected by mammography [16]. The patient was diagnosed with fibroadenoma. 360 scan lines of RF data were obtained from transducer and stored in MATLAB workspace. Fig. 4 shows plot of one scan line having 1600 samples, that are converted from floating point to fixed point numeric precision to control cost and consume less power.

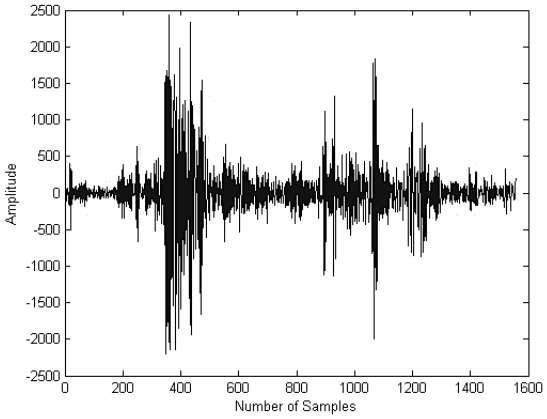

Fig. 4. RF scan line

With reference to Table I 32-tap filter provides least RMSE (0.0090), hence we implemented 32-tap FIR Hilbert filter having the magnitude response shown in Fig. 5 to obtain in-phase and quadrature phase components.

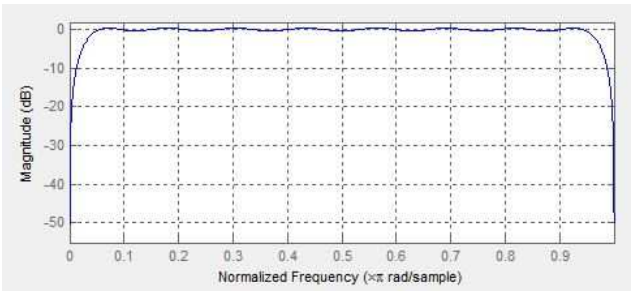

Fig. 5. Frequency response of 32-tap FIR Hilbert filter

Fig. 6 shows block diagram of envelope detection, onto which normalized RF scan line is passed. The quadrature components obtained from Hilbert filter block are passed through envelope detector to detect the envelope of the RF signal. Fig. 7 shows the envelope of input signal shown in Fig. 4

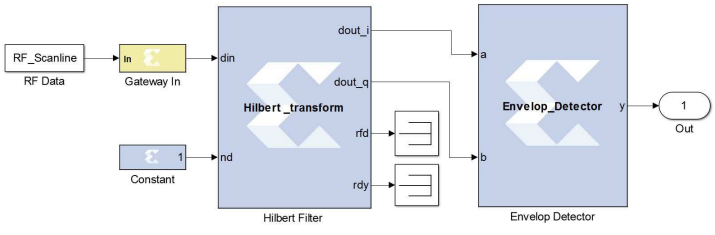

Fig. 6. Envlope detection block

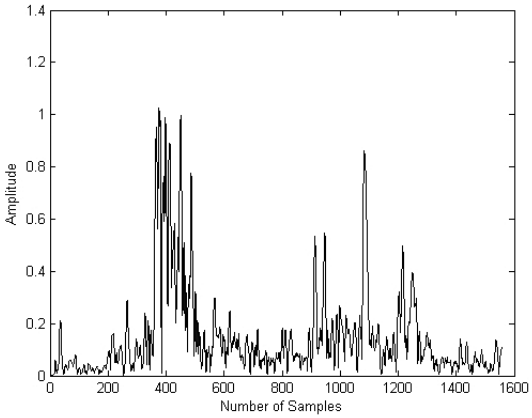

Fig. 7. Envelope detected data

Fig. 8 shows the block diagram of log compression technique using 16-KB look up table (LUT) to obtain the compressed data. Fig. 9 shows the log compressed data having less dynamic range compared to original data as in Fig. 7. Fig. 10 and Fig. 11 show images with and without log compression.

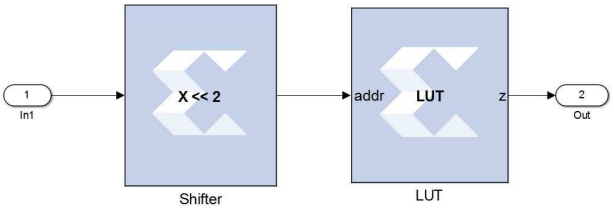

Fig. 8. Compression block

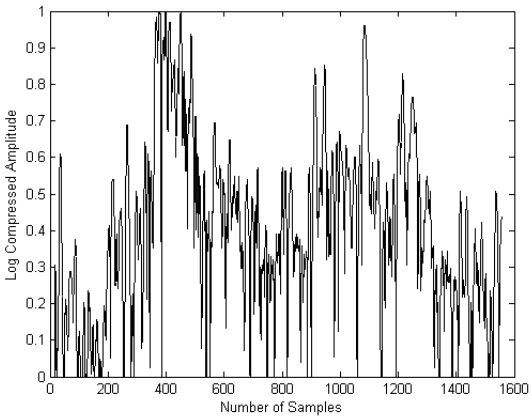

Fig. 9. Log compressed data

For the image construction, we mapped the log compressed data to their respective gray levels and displayed the final image as in Fig. 11. Later we applied our image enhancement technique which flattens the histogram and enhances the contrast of image, making it better than the traditional image developed on ultrasound machines. Fig. 12 shows the enhanced final image that was obtained.

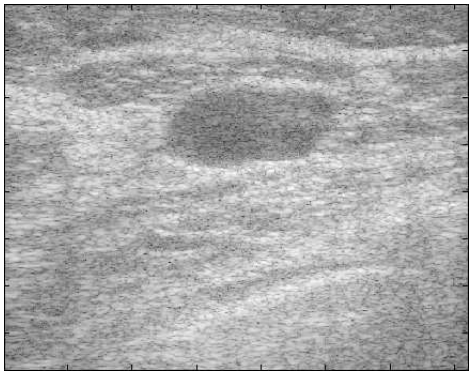

Fig. 10. Image without compression

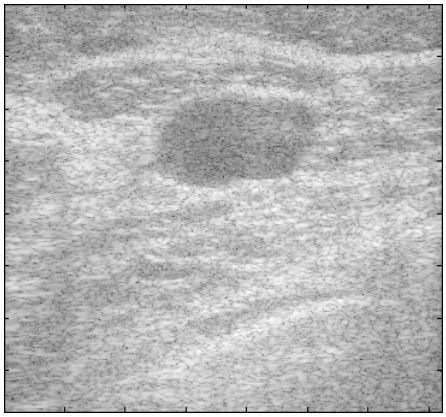

Fig. 11. Image after compression

Table.II gives the utilization summary for the whole implementation, the used devices, available in the port, and the utilization percentage using Kintex-7 FPGA.

V. Conclusion

In this paper, we were able to present the FPGA based ultrasound backend system that would process the echo signals received from tissues. While processing we were able to develop envelope detection block using 32-tap FIR Hilbert transform, log compression block to compress the dynamic range, interpolation to reduce the blocking artifacts and finally image quality is enhanced using full scale contrast stretch to give a better contrast than traditional ultrasound systems. Implementation on FPGA reduces the cost of development and also provides a platform for the researchers to develop new algorithms and implement them which can lead to a new era of ultrasound imaging.

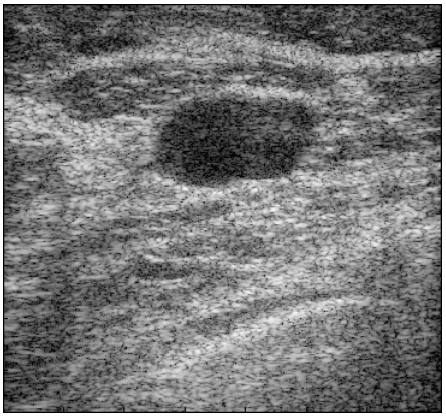

Fig. 12. Final image after enhancement

TABLE II
DEVICE UTILIZATION SUMMARY

Slice Logic Utilization	Used	Available	Utilization
Number of Slice Registers	1,902	407,600	1%
Number used as Flip Flops	1,902	-	-
Number of Slice LUTs	2,526	203,800	1%
Number used as logic	2,224	203,800	1%
Number using O6 output only	2,072	-	-
Number using O5 output only	8	-	-
Number using O5 and O6	144	-	-
Number used as Memory	296	64,000	1%
Number used as Shift Register	296	-	-
Number using O6 output only	296	-	-
Number used exclusively as route-thrus	6	-	-
Number with same-slice register load	6	-	-
Number of occupied Slices	798	50,950	1%
Number of LUT Flip Flop pairs used	2,611	-	-
Number with an unused Flip Flop	739	2,611	28%
Number with an unused LUT	85	2,611	3%
Number of fully used LUT-FF pairs	1,787	2,611	68%
Number of unique control sets	6	-	-
Number of Slice registers lost to control set restrictions	18	407,600	1%
Number of bonded IOBs	111	500	22%
Average Fanout of Non-Clock Nets	3.25	-	-

REFERENCES

[1] D. A. Christensen, *"Ultrasonic Bioinstrumentation,"* Jonh Wiley & Sons, New York, 1988.

[2] J. A. Zagzebski, *"Essentials of ultrasound physics,"* St Louis, Mo:Mosby, 1996.

[3] Standard [online]. Available: http://www.ultrasonix.com/ultrasound-systems/sonixtablet

[4] Peng Zhang, "Programmable-logic and application-specific integrated circuits," *Advanced Industrial Control Technology*, First ed. Kidlington, UK:Elsevier Inc., ch. 6, sec. 2, pp. 224-226, 2010.

[5] J. Ophir and N. J. Makland, "Digital scan converters in diagnostic ultrasound imaging," *Proc. IEEE*, vol. 67, no. 4, pp. 654-664, Apr. 1979.

[6] G. Wolberg, *"Digital Image Warping,"* Los Alamitos, CA: IEEE Comput. Soc. Press, 1990.

[7] S. Sikdar, R. Managuli, and Y. kim, "Programmable ultrasound scan conversion on a mediaprocessor-based sysem," *Proc. SPIE*, vol. 4319, pp. 699-711, May 2001.

[8] J. O. Smith, *"Mathematics of the Discrete Fourier Transform (DFT)"*, Center for Computer Research in Music and Acoustics (CCRMA), Department of Music, Stanford University, Stanford, California, 2002.

[9] A. V. Oppenheim and R.W.Schafer, *Discrete-Time Signal Processing"* NJ:Prentice-Hall,Englewood Cliffs, 1989.

[10] S. Sukittanon, S. G. Dame, FIR Filtering in PSoC^{TM} with Application to Fast Hilbert Transform, Cypress Semiconductor Corp., Cypress Perform, 2005.

[11] Mawia Ahmed Hassan and Yasser Mostafa Kadah, "Digital Signal Processing Methodologies for Conventional Digital Medical Ultrasound Imaging System," IEEE Trans *American Journal of Biomedical Engineering* [Online], 3(1), 14-30, 2013. Available:http://journal.sapub.opr/ajbe

[12] Szabo, T. L., *"Diagnostic Ultrasound Imaging: Inside Out,"* Elsevier Academic Press: Hartford, Connecticut, 2004.

[13] R. C. Gonzalez, R. E. Woods, *"Digital Image Processing,"* Pearson Prentice Hall, Upper Saddle River, New Jersey, 2008

[14] Richard WD, Arthur RM, "Real-time ultrasonic scan conversion via linear interpolation of oversampled vectors," *Ultrason Imag.*, vol. 16, no. 2, 109-123, 1994.

[15] Standard [online]. Available: http://www.xilinx.com/products/silicon-devices/fpga/kintex-7

[16] Standard [online]. Available: http://ultrasonics.bioengineering.illinois.edu/data_patient.asp